



ELSEVIER

Available online at [www.sciencedirect.com](http://www.sciencedirect.com)

SCIENCE @ DIRECT®

Deep-Sea Research I 50 (2003) 1189–1203

DEEP-SEA RESEARCH  
PART I

[www.elsevier.com/locate/dsr](http://www.elsevier.com/locate/dsr)

# Chlorophyll *a* and nitrogen flux in the tropical North Atlantic Ocean

Nixon Bahamón\*, Zoila Velásquez, Antonio Cruzado

*Centre d'Estudis Avançats de Blanes, Carrer d'accés a la Cala Sant Francesc 14, E-17300 Blanes, Spain*

Received 4 February 2002; received in revised form 27 February 2003; accepted 13 August 2003

## Abstract

The phytoplankton chlorophyll *a* concentration and spatial distribution, and upward nitrogen transport toward the productive zone as controlled by the vertical turbulent diffusion and nitrate gradients, were evaluated along a 24.5° latitude section in the North Atlantic Ocean. The diffusive nitrate flux reasonably explained the expected new production in the Western Sargasso (WS), Central Sargasso (CS) and Eastern Atlantic (EA). The average upward nitrogen flux in those areas was 0.53 mmol N m<sup>-2</sup> day<sup>-1</sup> (±0.04 SE), representing from 0.23 to 0.34 of the total primary production. In the Canary Current (CC) zone, the estimates of upward nitrogen flux did not explain the expected new production, which appears to depend on laterally advected nutrients from coastal upwelling. In the CC, the nitracline depth was highly variable around ~80 m depth, being more constant in the other zones around 136 m depth. The thermocline was located at depths between 28 and 44 m along the whole area except in some stations in the CC, where the upwelling system broke up the thermocline. The depth of the 26.0 isopycnal closely related to nitracline depth was always greater than that of the thermocline in the CS, EA and CC zones. In WS, the depth of the 26.0 isopycnal was highly variable responding to local subthermocline oscillations, while the nitracline remained relatively constant around 1% surface PAR depth, thus suggesting PAR as responsible instead of density for the top depth of the nitracline. Typical depth-integrated phytoplankton chlorophyll *a* inventories around 24 mg m<sup>-2</sup> showed an average deep maximum of 0.27 mg m<sup>-3</sup> at ~119 m depth in all zones, except in the CC, where the chlorophyll *a* inventory was 32 mg m<sup>-2</sup> with an average maximum concentration around 0.39 mg m<sup>-3</sup> at ~80 m depth. The variability of the upward diffused nitrogen was better explained by the nitrate gradient ( $n = 86$ ,  $r^2 = 0.76$ ;  $P < 0.01$ ) than by the diffusion term ( $n = 86$ ;  $r^2 = 0.12$ ;  $P < 0.01$ ). This suggests that the nitrogen fluxes are more dependent on the nitrate gradients at the nitracline than on the density gradients regulating turbulent diffusion.

© 2003 Elsevier Ltd. All rights reserved.

**Keywords:** Nitrogen flux; Chlorophyll *a*; Thermocline; Nitracline; Turbulent diffusion; WOCE

## 1. Introduction

In the upper waters of the open ocean, the interaction of phytoplankton with physical and biogeochemical processes is relevant to global climate change and the carbon cycle, because of the role played by these ecosystems in regulating

\*Corresponding author. Tel.: +34-972-336101; fax: +34-972-337806.

E-mail address: bahamon@ceab.csic.es (N. Bahamón).

fluxes of matter between the atmosphere and deeper waters. In the euphotic zone, assumed here to be the water layer above 1% of the surface irradiance, phytoplankton converts inorganic carbon into organic matter, part of which (a highly variable fraction around 30%) is exported toward deeper waters where most of the regeneration of nutrients takes place. This downward flux is roughly compensated by the upward transport of nutrients to the surface contributing to support a year round cycle of primary production (Platt and Harrison 1985; McGillicuddy and Robinson, 1997). The primary production of phytoplankton based on these nutrients (nitrate) is called new production, in opposition to the regenerated production from nitrogen recycled from organic matter (ammonium) within the productive zone (Dugdale and Goering, 1967; Eppley and Peterson, 1979).

The upward diffused nitrogen regulated by the water density and the nitrate gradients contribute to control the spatial distribution of the phytoplankton (Menzel and Ryther, 1960; Eppley and Peterson, 1979). Above the pycnocline (maximum density gradient), surface wind stress is often assumed to be the main source of energy for turbulent mixing. Below the pycnocline, turbulent diffusion is the result of complex hydrographic mechanisms with decreasing buoyancy and internal wave breaking being held responsible for the vertical turbulence mixing (Gaspar et al., 1990). The buoyancy frequency is a density-dependent measure of vertical stability of the water layer, with lower values indicating a higher stability as occurs at the pycnocline, and higher values indicating weaker stability as occurs both in the surface mixed layer and in deep waters with small density gradients. As a result, the turbulent diffusion is expected to be inversely proportional to the buoyancy frequency with maximum values in the mixed layer and minimum within the pycnocline. Various ecological models use this vertical structure as a framework to better understand processes related to phytoplankton chlorophyll in oligotrophic environments such as the western Mediterranean and tropical North Atlantic (Varela et al., 1994; Zakardjian and Prieur, 1998; Bahamón and Cruzado, 2003).

In eddy-induced upwelling areas, the upward advection is responsible for transporting nutrients to the surface, fuelling new production (McGillicuddy and Robinson, 1997). Temperate waters are fertilized during the winter convection that forces homogenization of depleted surface waters with nutrient-rich intermediate waters (Kiefer and Kremer, 1981). Typically, oligotrophic tropical waters show a pycnocline linked to the permanent thermocline, which acts as a physical barrier regulating the vertical transport of nutrients by a strong reduction of the diffusive flux. In the North Atlantic Ocean, the 17–19°C isotherms, near the surface in the Guinea Dome, appear somewhat deeper near 10°N because of the link to the upwelling off northwest Africa and the divergence of water masses. The 17–19°C isotherms sink to depths between 150 and 250 m at latitudes between 20° and 30° north and south, being deeper in the southern than in the northern hemisphere (Mayer et al., 1998). Isotherm oscillations have been pointed out to be closely linked to the position of the deep chlorophyll maximum (DCM), located below the depth of maximum stability and receiving between 3% and 1% of surface irradiance (Bricaud et al., 1992; Agusti and Duarte, 1999).

In the stratified tropical North Atlantic, the upward nitrogen fluxes toward the euphotic zone and primary production have close correlation with the maximum nitrate gradient (nitracline) (Herbland and Voituriez, 1979; Cullen and Epply, 1981; Bahamón, 2002). Estimates of nitrogen fluxes to the euphotic layer in the tropical North Atlantic range from 0.1 to 0.8 mmol m<sup>-2</sup> day<sup>-1</sup>, depending on the site and the method followed for estimating. For example, Lewis et al. (1986) estimated an upward nitrogen flux of 0.14 mmol m<sup>-2</sup> day<sup>-1</sup> at 28°N, 23°W, by using direct measurements of turbulent diffusion and nitrate gradients. Planas et al. (1999) gave average estimates of nitrogen flux around 0.74 mmol m<sup>-2</sup> day<sup>-1</sup> along 16–27°N, 28°W using a parameterization of the vertical turbulence and nitrate gradients. Gruber and Sarmiento (1997) gave nitrate flux estimates of 0.2 mmol m<sup>-2</sup> day<sup>-1</sup> in the tropical and subtropical North Atlantic, based on linear combinations of nitrate and phosphate distribution in the area.

Even though the density and nitrate distributions in the vertical regulate the chlorophyll distribution and abundance in the ecosystem, there are other important mechanisms controlling the chlorophyll dynamics, such as the differential plankton sinking rates, physiological changes in the carbon to chlorophyll *a* ratio and differential grazing by zooplankton, among others (Longhurst and Harrison, 1989). All the mechanisms controlling the chlorophyll distribution still need to be better studied in order to provide understanding and quantification of the complex ecological interactions around primary producers (Furuya, 1990; Zakardjian and Prieur, 1998; Goericke and Welschmeyer, 1998).

The present work is based on oceanographic information from a transatlantic section carried out during summer 1992 (WOCE A5 section), from northwest Africa (16°W) to the Bahamas (75°W) along 24.5°N (Parrilla et al., 1994; Garcia et al., 1998). The area covered by the section is governed by hydrographic regimes driving the southern part of the subtropical anticyclonic gyre. On the western side near the Bahamas, large oscillations of currents take place induced by intense frontal structures in the North Equatorial Current. To the east, near Africa, the southward Canary current, merging with the North Equatorial Current off Africa, appears relatively weak and diffuse, generating coastal upwelling of intermediate waters (Schmitz and McCartney, 1993). Yearly observations of both hydrographic and biogeochemical properties in the study area allow differentiation of specific areas or biogeochemical provinces (Longhurst et al., 1995; Sathyendranath et al., 1995). The present section crossed the southern parts of three distinct biogeochemical provinces: West Gyre, East Gyre and Canary Current. The west-gyre province includes the poleward part of the anticyclonic gyre from the western boundary current to the Mid-Atlantic Ridge (at about 50°W). The east-gyre province is a continuation of the western province from the Mid-Atlantic Ridge to the Canary Current boundary in the east. The Canary Current province, characterized by coastal upwelling, includes the eastern boundary current from Galicia (Spain) to Cape Verde in North Africa. Primary production

in the three provinces increases eastward with values around 114, 174 and 600 g C m<sup>-2</sup> yr<sup>-1</sup>, respectively (Longhurst et al., 1995; Sathyendranath et al., 1995).

In this study the vertical variability of both density and nitrate concentrations in the upper layers of the tropical North Atlantic are evaluated with regard to the spatial distribution of chlorophyll and the upward nitrogen flux to the euphotic zone. Estimates of new production are given on the basis of nitrogen fluxes. The zonal variability of physical and biogeochemical properties is examined in order to explain differences in the vertical profiles of chlorophyll *a*. It is maintained that the phytoplankton chlorophyll and new production in tropical North Atlantic waters are controlled mainly by nitrate fluxes across the nitracline with a minor influence of the thermocline.

## 2. Data sources and processing

### 2.1. Oceanographic cruise

The *WOCE A5* North Atlantic cruise was conducted on board the *BIO Hespérides* from July 12th to August 15th 1992, as part of the *WOCE* Program (Fig. 1). The data from the cruise used in this work were compiled by the CEAB/CSIC Chemical Oceanography Group and submitted to the *WOCE* Program Office, a component of the World Climate Research Program. Data are also available at <http://www.ceab.csic.es/~oceanlab/>. AC and ZV made on board measurements of nitrite, nitrate and chlorophyll *a*. A total of 101 full-depth oceanographic stations were occupied. The average distance between stations was approximately 59 km over the entire section covering a total of around 5960 km. The present work was limited to the upper 500 m. Typically, 121 Niskin bottle samples were taken. Bottles triggered above 300 m depth were used for chlorophyll *a* analysis. CTD data were 3 m depth-averaged from surface to bottom.

### 2.2. Dissolved inorganic nutrients and chlorophyll *a*

Nitrite + nitrate (μmol kg<sup>-1</sup>), hereafter called simply nitrate, were measured according to

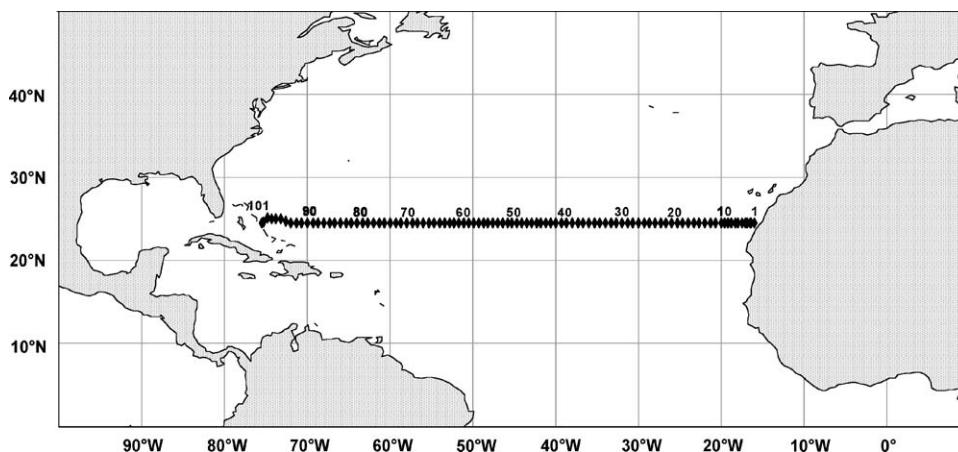


Fig. 1. Locations of the 101 oceanographic stations on the WOCE-A5 transatlantic section along 24.5°N. Average distance between stations was 59 km with small variations along the entire section.

Whitledge et al. (1981). The precision of data was 0.2 and 0.3  $\mu\text{mol kg}^{-1}$  ( $\pm 1$  SD) in the eastern and western Atlantic, respectively (García et al., 1998).

Chlorophyll *a* was estimated from non-fractionated particulate matter. Water samples 0.5–3.0 l were filtered through 4.7 cm Whatman GF/F filters that were kept frozen for about 24 h and then processed on board. The phytoplankton pigments were determined by the spectrophotometric technique of Jeffrey and Humphrey (1975) after extraction for more than 24 h with 5 ml acetone (90%) and centrifugation of the resulting suspension at 3000 rpm for 30 min. The absorbances were read in the supernatant at 750, 664, 647 and 630 nm. Although chlorophyll *b* and *c* are deduced from the equations used, only chlorophyll *a* values are used in this paper, since it is a more accurate estimator of the phytoplankton biomass (Jeffrey and Welschmeyer, 1997).

In order to evaluate the vertical distribution of chlorophyll as a function of photosynthetically available radiation (PAR), the surface solar irradiance was taken as 900  $\text{W m}^{-2}$  at noon (Bricaud et al., 1992), 46% of such irradiance being PAR (Baker and Frouin, 1987). PAR was assumed to decline with depth  $z$  because of pure water absorption ( $K_w$ ) and phytoplankton self-shading ( $K_c$ ) as follows:  $\text{PAR}_{(z,t)} = \text{PAR}(0,t) \exp^{-Z(k_w+k_c \cdot [\text{PHY}])}$ , where  $K_w = 0.040 \text{ m}^{-1}$ ,  $K_c = 0.015 \text{ m}^2 (\text{mg Chl } a)^{-1} \text{ m}^{-3}$  ;

PHY is chlorophyll *a* in  $\text{mg m}^{-3}$ . This parameterization of PAR has been successfully used in ecological models of stratified environments in the NW Mediterranean and in the NE Atlantic (Bahamón and Cruzado, 2003).

### 2.3. Estimates of diffusive nitrogen fluxes

In order to estimate diffusive nitrogen fluxes, vertical turbulent diffusion was parameterized according to Osborn (1980). This parameterization method allows computation of turbulent diffusion values from vertical density gradients. Thus, an increase of the density gradient promotes higher stability of a water layer with lower turbulent diffusion rates (Zakardjian and Prieur, 1988; Helguen et al., 2002). The vertical flux of nitrate due to turbulent diffusion in the nitracline is the product of the nitrate gradient and the diffusion coefficient, the latter calculated as  $K_{(z)} = 0.25\varepsilon_{(z)}/N^2(z)$ , where  $N^2$  ( $\text{s}^{-2}$ ) is the Brunt-Väisälä buoyancy frequency  $N^2_{(z)} = (-g/\rho_w)(\partial\rho/\partial z)$  (Millard et al., 1990);  $\varepsilon_{(z)}$  is the turbulent kinetic energy (TKE) dissipation rate at a given depth;  $g$  is gravity acceleration ( $9.82 \text{ ms}^{-2}$ );  $\rho_w$  is density ( $\text{kg m}^{-3}$ ); and  $\partial\rho/\partial z$  is the vertical density gradient. The density anomaly ( $\sigma_\theta, T, S, 0$ ) was calculated following Millero and Poisson (1981). TKE links the turbulent regime and stratification in the water column and is assumed to be  $4\text{E-}07 \text{ m}^2 \text{ s}^{-3}$  in the

mixing layer but to decrease exponentially downward until it reaches a background value of  $4\text{E-}08\text{ m}^2\text{ s}^{-3}$  (Varela et al., 1994; Zakardjian and Prieur, 1998; Bahamón and Cruzado, 2003).  $N^2$  and  $K_z$  profiles were smoothed by the nearest neighbor gridding method, in which the value of the nearest datum is assigned to each grid node.

### 3. Results

#### 3.1. Physical properties

Sea surface temperature increased by  $\sim 10^\circ\text{C}$  from east to west, the warmer surface waters being near the Bahamas ( $\sim 29^\circ\text{C}$ ) and the colder waters near Africa ( $\sim 19^\circ\text{C}$ ; Fig. 2a). The top of the thermocline was found at depths between 23 and 69 m along the whole section, except east of  $17^\circ\text{W}$ , where there was outcropping of colder, nutrient-rich waters induced by coastal upwelling in the Canary Current. A large surface lens of salty water with values between 37.0 and 37.6 was observed between  $25$  and  $58^\circ\text{W}$  (Fig. 2b), attributed to the injection of salty surface waters by the subtropical gyre outcrop (Kawase and Sarmiento, 1985). This lens does not significantly alter the longitudinal dipping of isopycnals (Fig. 2c), which follow the isotherms. A deepening of the 26.0 isopycnal from the surface on the east side to  $\sim 200$  m depth on the west side of the section was remarkable. At  $42$ – $43^\circ\text{W}$ , it crossed the 1% PAR contour at a depth of  $\sim 120$  m and remained between 1% and 0.1% PAR contours all the way to  $65^\circ\text{W}$  (Fig. 3). West of this longitude, subthermocline isopycnal oscillations reflected the existence of eddies, and the 26.0 isopycnal was often below the 0.1% PAR level. Two relatively strong surface horizontal density gradients (isopycnal fronts) were observed, one near Africa in the upwelling area and the other around the center of the section, between  $51$  and  $54^\circ\text{W}$  longitude.

As observed from density, the vertical distribution of  $N^2$  (Fig. 4a) confirmed the existence of subthermocline instabilities (oscillations) near the Bahamas. The largest values of  $N^2$ , indicating the highest stability, were found around the thermo-

cline. In the mixed layer above the thermocline,  $N^2$  showed lower values along the whole section. Below the thermocline,  $N^2$  appeared scattered in the western basin, with smaller values alternating with higher values. The  $K_z$  distribution pattern (Fig. 4b), opposite to that of  $N^2$ , is highly variable with values increasing in the low stability stations. Larger values of  $K_z$  found above the thermocline contrasted with low values at the thermocline. Turbulent diffusion increases toward the bottom boundary, reaching nearly three times the values at the thermocline.

#### 3.2. Biogeochemical properties

Typical nutrient-depleted waters were observed not only above the thermocline but also at depths far below it (Fig. 5). The  $0.5\ \mu\text{mol kg}^{-1}$  nitrate closely corresponding to the nitracline was positioned between 120 and 160 m depth around the 1% surface PAR in most of the section, except near Africa where it was positioned between 70 and 90 m depth. A subsurface wedge of high nitrate water was noticeable in the Canary Current area extending westward from the African side ( $16.6^\circ\text{W}$ ) to about  $25^\circ\text{W}$ , suggesting fertilization from nutrient-rich coastal waters. Nutrients below the euphotic zone showed important longitudinal variability since their concentrations near Africa were approximately twice those observed near the Bahamas.

A continuous chlorophyll *a* maximum layer ( $>0.15\ \text{mg Chl } a\ \text{m}^{-3}$ ) was observed over the entire section (Fig. 3). The depth of DCM was rather stable around 110–140 m, between the 2% and 0.1% PAR depth, except at stations east of  $24^\circ\text{W}$  where the DCM was positioned around 80 m depth closer to 10% PAR level. The average percentage irradiance at the DCM close to the nitracline depth in the entire section, except near Africa, was around  $0.8 \pm 0.2$  SE the surface PAR. The upper boundary of the DCM is close to the surface east of  $25^\circ\text{W}$  and deepens to 98 m depth west of  $35^\circ\text{W}$ . The depth of the lower boundary varied between 95 and 160 m at the same longitudes. Chlorophyll *a* was scattered in various layers of the density field, but chlorophyll *a* was not higher than  $0.15\ \text{mg m}^{-3}$  below the  $24.3\sigma_\theta$

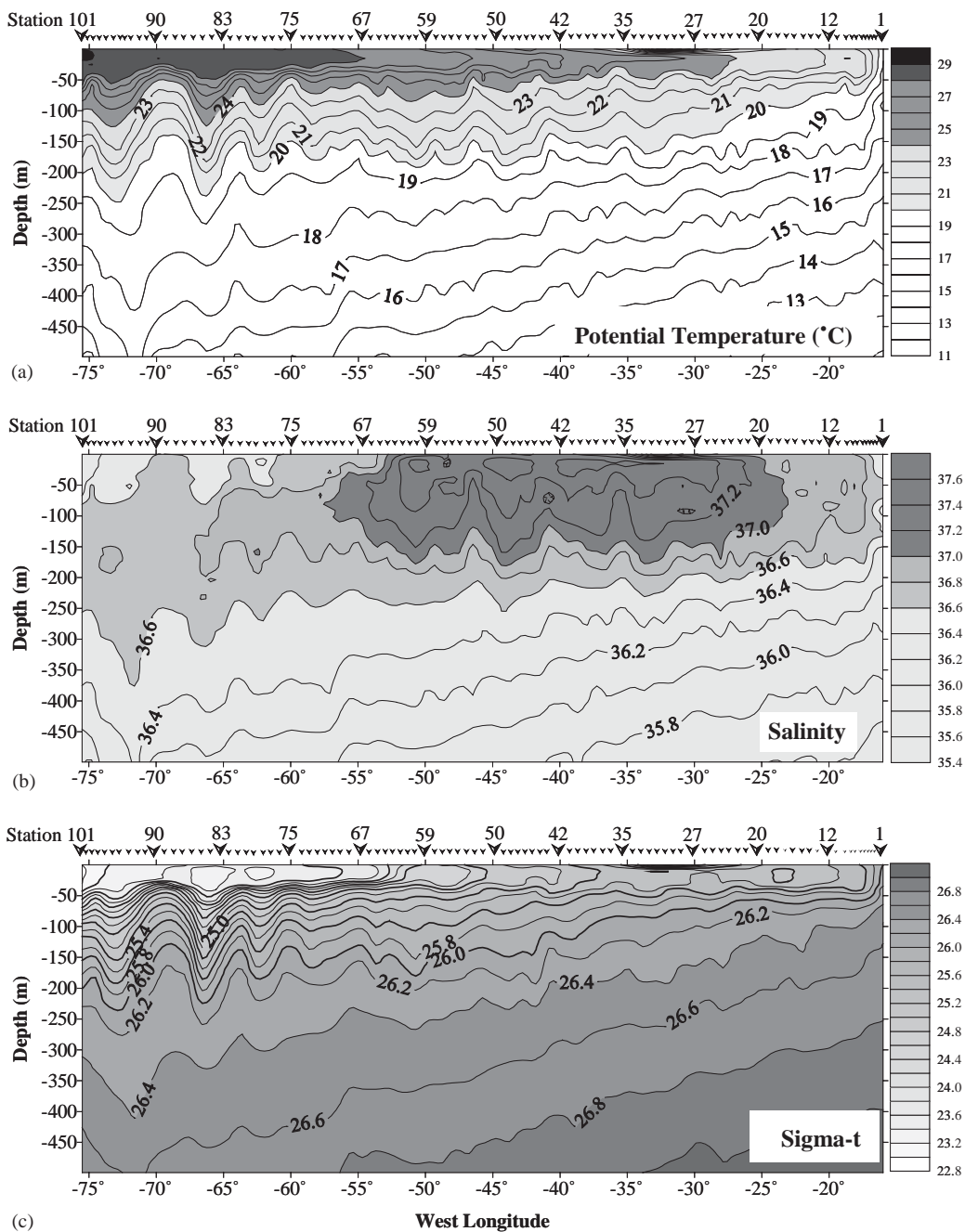


Fig. 2. Longitudinal distribution of (a) temperature (°C), (b) salinity and (c)  $\sigma_\theta$  ( $\text{kg m}^{-3}$ ) in the upper subtropical north Atlantic. 16,766 data points were used to build contours (101 stations, each one with 166 depth-averaged data points).

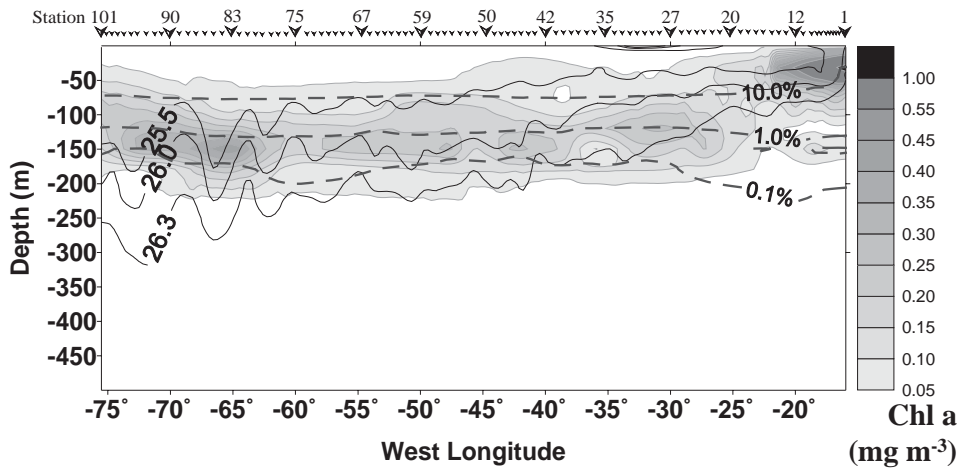


Fig. 3. Longitudinal distribution of chlorophyll *a* ( $\text{mg m}^{-3}$ , shadowed contours) with reference isolines of irradiance (%PAR, dashed dark lines) and  $\sigma_\theta$  ( $\text{kg m}^{-3}$ , continuous dark lines).

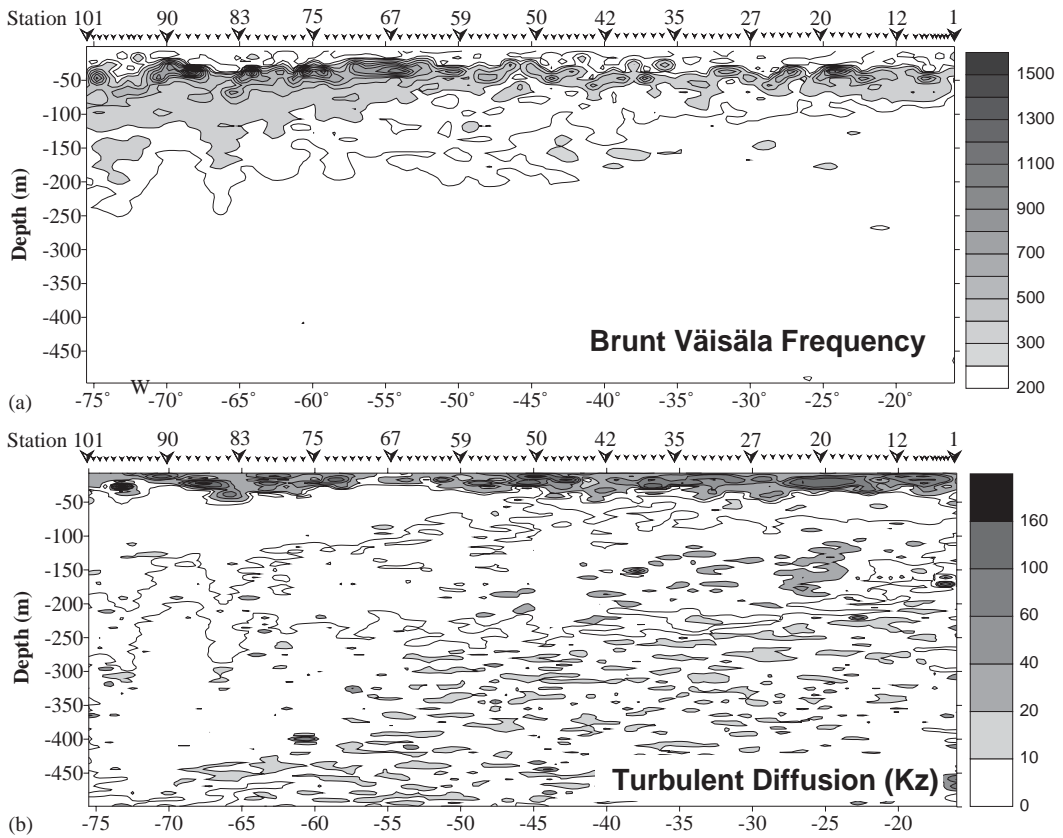


Fig. 4. Longitudinal distribution of (a) the Brunt–Väisälä frequency ( $N^2, \text{s}^{-2}$ ) with scale modified only for contouring purpose ( $N^2 \times 10^6 + 200$ ), (b) vertical turbulent diffusion coefficient ( $K_z, \text{m}^2 \text{day}^{-1}$ ), calculated from  $N^2$ , following the Osborn (1980) formulation.

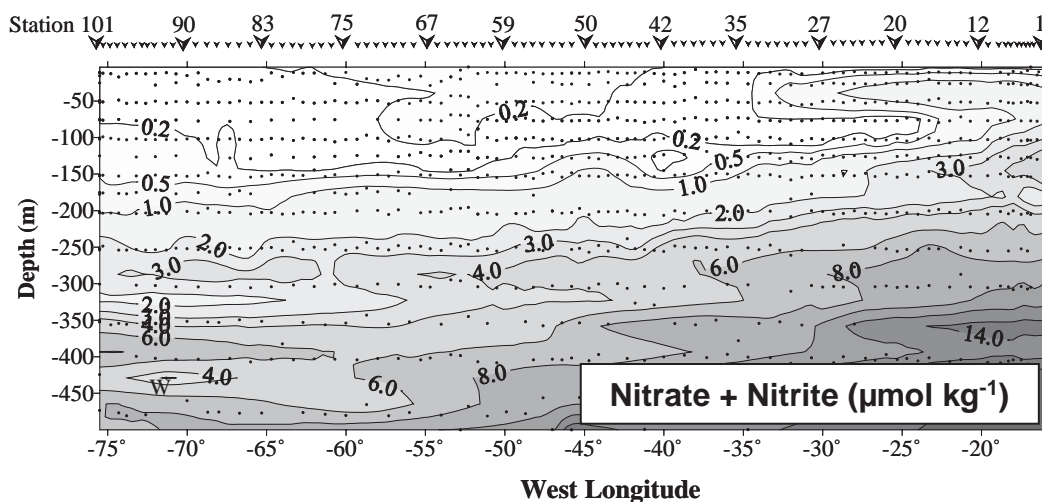


Fig. 5. Longitudinal distribution of nitrogen: nitrate + nitrite ( $\mu\text{mol kg}^{-1}$ ). Points indicate sampling depths.

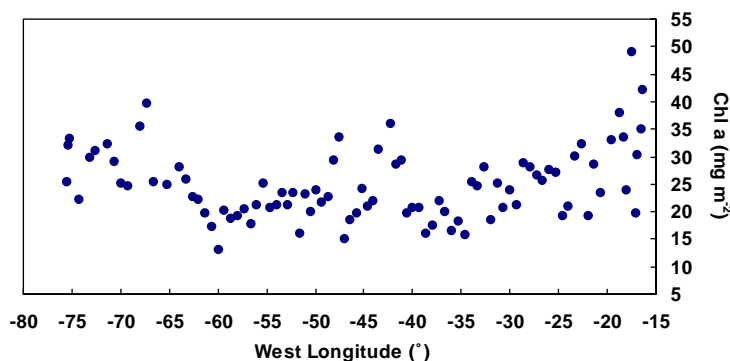


Fig. 6. Depth-integrated chlorophyll *a* ( $\text{mg m}^{-2}$ ) in all the stations on the WOCE A5 section.

level, corresponding to surface waters in the western basin (west of  $58^\circ\text{W}$ ) (Fig. 2c). Various chlorophyll *a* maxima were observed inside the continuous maximum chlorophyll *a* layer at both east and west extremes of the section and at the center.

At most of the stations, depth-integrated chlorophyll *a* (Fig. 6) ranged between 15 and  $30\text{ mg m}^{-2}$ . Chlorophyll *a* exceeded this range at stations located at the eastern and western boundaries (west  $67^\circ$  and east  $24^\circ\text{W}$ ) and at stations in the center of the section (between  $41^\circ$  and  $49^\circ\text{W}$ ) showing the highest chlorophyll concentrations at the DCM (Fig. 3).

### 3.3. Regional differences

The section was divided into four zones according to the vertical distributions of chlorophyll *a* (Fig. 7). Western Sargasso (WS) ( $75.5^\circ\text{--}58.0^\circ\text{W}$ ) had surface chlorophyll lower than  $0.1\text{ mg m}^{-3}$  and a broad maximum around  $0.3\text{ mg m}^{-3}$  at  $\sim 127\text{ m}$  depth. Central Sargasso (CS) ( $57.3^\circ\text{--}47.6^\circ\text{W}$ ) showed surface chlorophyll *a* similar to that of WS ( $<0.1\text{ mg m}^{-3}$ ) with a maximum of about  $0.24\text{ mg m}^{-3}$  at  $\sim 141\text{ m}$  depth. In comparison with CS, Eastern North Atlantic (EA) ( $47.0^\circ\text{--}24.0^\circ\text{W}$ ) showed a higher surface chlorophyll of about  $0.15\text{ mg m}^{-3}$  and vertical profiles with diffuse

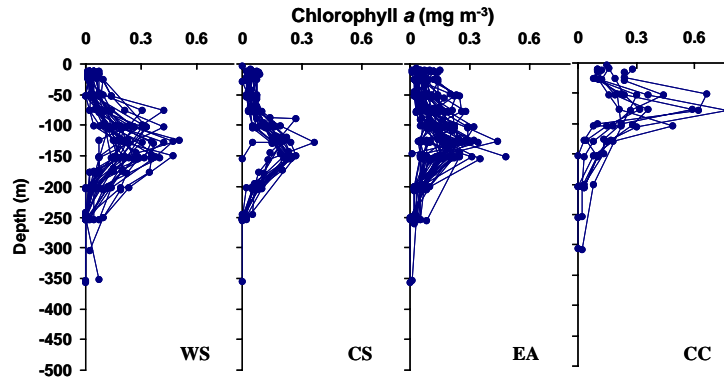


Fig. 7. Chlorophyll *a* grouped in four areas with apparently different vertical distributions. WS = Western Sargasso (75.5–58.0°W); CS = Central Sargasso (57.3–47.6°W); EA = Eastern Atlantic (47.0–24.0°W), CC = Canary Current (23.3–16.0°W).

maxima around  $0.25 \text{ mg m}^{-3}$  at a shallower depth at  $\sim 118 \text{ m}$ . Finally, the Canary Current area (CC) ( $23.3^{\circ}$ – $16.0^{\circ}$ W) held the highest average chlorophyll maximum around  $0.4 \text{ mg m}^{-3}$  at the shallowest chlorophyll *a* maximum depth ( $\sim 79 \text{ m}$ ). WS, CS and EA will be further referred to as the trade-wind domain.

Physical and biogeochemical properties of the four zones were analyzed (Table 1), some of them showing statistically significant differences (Fig. 8). As expected, the CC was the area with the largest differences from areas along the section. The analysis of variance showed that in the CC both the maximum chlorophyll concentration and the integrated chlorophyll were significantly higher than in the other zones. The depths of the chlorophyll maximum and the nitracline were shallower. Along the section, the nitrate gradient showed a clear decrease westward. Nitrate gradient in WS was the smallest of all. The integrated chlorophyll *a* values were similar in all three trade-wind areas, but the DCM showed significant differences. The deepest DCM was found in CS with a shallower thermocline (and pycnocline) than in WS. Turbulent diffusion at the nitracline depth was significantly higher in EA than in the other zones. The upward diffused nitrate flux was significantly higher in EA than either in CS and WS. In the CC, the average upward nitrate flux was lower than expected from the higher nitrate gradient, explained by the very low values of turbulent diffusion.

#### 4. Discussion

The thermocline depth in the trade-wind domain (WS, CS, EA) was relatively steady around 30–40 m. The chlorophyll *a* maximum was located far below the thermocline, close to the nitracline at  $\sim 130 \text{ m}$  depth. Thermocline waters were characterized by low nutrient and chlorophyll concentrations, below the detection limit, making the role played by isopycnal fronts in transporting nutrients undetectable and, therefore, hardly modifying the chlorophyll distribution. This was the case of the isopycnal front between  $51$  and  $54^{\circ}$ W, which showed no apparent influence on the chlorophyll *a* concentrations. In the CC, relatively high concentrations of chlorophyll *a* spread from subsurface to about 100 m depth as a response to horizontal nutrient wedges coming from the coast to about 800 km offshore.

Nitrate concentration was low in surface waters and increased with depth. The maximum gradient (nitracline) was found at the 26.0 isopycnal (Fig. 9). The nitracline became deeper in the EA and CS, but not in WS. Near the Bahamas, the depth of the 26.0 isopycnal was quite variable while the nitracline was nearly constant. The 26.0 isopycnal often crossed the 1% of surface irradiance depth at  $\sim 120 \text{ m}$  as a response to subthermocline oscillations attributed to a decrease in buoyancy and breaking of internal waves (Gaspar et al., 1990). Even though the nitrate concentration did not show a considerable

Table 1  
Basic statistics of summer physical and biogeochemical features of upper North Atlantic waters along 24.5°N

	WS ( <i>N</i> = 23)		CS ( <i>N</i> = 17)		EA ( <i>N</i> = 37)		WS+CS+EA ( <i>N</i> = 77)		CC ( <i>N</i> = 13)	
	Mean	SE	Mean	SE	Mean	SE	Mean	SE	Mean	SE
Thermocline gradient (°C m <sup>-1</sup> )	0.331 ± 0.031		0.273 ± 0.015		0.246 ± 0.011		0.281 ± 0.024		0.194 ± 0.021	
Depth of thermocline (m)	41 ± 3		30 ± 2		37 ± 2		36 ± 2		40 ± 3	
Density gradient at pycnocline (kg m <sup>-4</sup> )	0.104 ± 0.010		0.086 ± 0.005		0.062 ± 0.003		0.083 ± 0.003		0.055 ± 0.005	
Depth of pycnocline (m)	43 ± 3		30 ± 2		37 ± 1		36 ± 2		38 ± 3	
Buoyance frequency maximum (s <sup>-1</sup> )	0.028 ± 0.001		0.026 ± 0.001		0.022 ± 0.001		0.025 ± 0.001		0.021 ± 0.001	
Depth of buoyance frequency maximum (m)	49 ± 3		35 ± 2		42 ± 2		42 ± 2		44 ± 2	
<i>K<sub>z</sub></i> at the nitracline depth (m <sup>2</sup> day <sup>-1</sup> )	16.54 ± 0.50		22.02 ± 0.78		27.36 ± 1.86		21.98 ± 0.80		18.14 ± 1.78	
Nitrate gradient at nitracline depth (mmol N m <sup>-4</sup> )	0.013 ± 0.002		0.022 ± 0.003		0.033 ± 0.004		0.023 ± 0.003		0.045 ± 0.011	
Depth of the top of nitracline (m)	132 ± 6		149 ± 8		130 ± 6		136 ± 3		80 ± 4	
Integrated chlorophyll <i>a</i> (mg m <sup>-2</sup> )	25.8 ± 1.3		22.7 ± 1.0		22.9 ± 0.8		23.9 ± 0.5		31.6 ± 2.4	
Chlorophyll <i>a</i> maximum (mg m <sup>-3</sup> )	0.30 ± 0.02		0.24 ± 0.01		0.25 ± 0.01		0.27 ± 0.01		0.39 ± 0.05	
Depth of chlorophyll <i>a</i> maximum (m)	127 ± 6		141 ± 5		118 ± 5		129 ± 3		79 ± 6	
Nitrate flux at nitracline (mmol N m <sup>-2</sup> day <sup>-1</sup> )	0.223 ± 0.026		0.504 ± 0.040		0.913 ± 0.073		0.526 ± 0.039		0.866 ± 0.101	
New primary production (mg C m <sup>-2</sup> day <sup>-1</sup> )	18.5 ± 2.0		40.7 ± 3.2		72.9 ± 5.7		42.7 ± 3.1		70.1 ± 7.8	

Areas indicated in the columns are Western Sargasso (WS) (75.5–58.0°W), Central Sargasso (CS) (57.3–47.6°W), Eastern Atlantic (EA) (47.0–24.0°W), and Canary Current (CC) (23.3–16.0°W). The oceanographic stations were numbered westward from NW Africa (St. 1) to the Bahamas (St. 101). Station numbers in each section are (WS) 72–101; (CS) 55–71; (EA) 18–54; (WS+CS+EA) 18–101; (CC) 1–17.

	WS	CS	EA	CC	
WS	■	■	■	■	Chlorophyll a maximum ( $\text{mg m}^{-3}$ ) Depth-integrated chlorophyll a ( $\text{mg m}^{-2}$ ) Depth at top of nitracline (m)
CS	■	■	■	■	
EA	■	■	■	■	
CC	■	■	■	■	
WS	■	■	■	■	Depth of chlorophyll a maximum (m)
CS	■	■	■	■	
EA	■	■	■	■	
CC	■	■	■	■	
WS	■	■	■	■	Nitrate gradient at top of nitracline ( $\text{mmol N m}^{-4}$ )
CS	■	■	■	■	
EA	■	■	■	■	
CC	■	■	■	■	
WS	■	■	■	■	Nitrate flux at nitracline ( $\text{mmol N m}^{-2} \text{d}^{-1}$ ) Nitrate-based PP ( $\text{mg C m}^{-2} \text{d}^{-1}$ )
CS	■	■	■	■	
EA	■	■	■	■	
CC	■	■	■	■	
WS	■	■	■	■	Thermocline gradient ( $^{\circ}\text{C m}^{-1}$ )
CS	■	■	■	■	
EA	■	■	■	■	
CC	■	■	■	■	
WS	■	■	■	■	Depth of thermocline (m)
CS	■	■	■	■	
EA	■	■	■	■	
CC	■	■	■	■	
WS	■	■	■	■	Depth of pycnocline (m)
CS	■	■	■	■	
EA	■	■	■	■	
CC	■	■	■	■	
WS	■	■	■	■	Density gradient at pycnocline ( $\text{kg m}^{-2}$ ) Brunt-Väisälä maximum ( $\text{s}^{-1}$ )
CS	■	■	■	■	
EA	■	■	■	■	
CC	■	■	■	■	
WS	■	■	■	■	Depth of B-V maximum (m)
CS	■	■	■	■	
EA	■	■	■	■	
CC	■	■	■	■	
WS	■	■	■	■	Turbulent diffusion coefficient at the nitracline depth ( $\text{m}^2 \text{d}^{-1}$ )
CS	■	■	■	■	
EA	■	■	■	■	
CC	■	■	■	■	

Fig. 8. Results of the analysis of variance (ANOVA) of selected physical and biogeochemical features in the tropical North Atlantic. Grey-shadowed squares indicate areas with significant differences ( $p < 0.05$ ). Since  $F$  was significant from the ANOVA test, a post hoc comparison of means was made using the Tukey honest significant difference test to determine which means contributed to this effect. WS = Western Sargasso, CS = Central Sargasso, EA = Eastern Atlantic, CC = Canary Current.

increase, subthermocline oscillations could play an important role in the formation of chlorophyll patches observed at 64, 69 and 75°W (Fig. 6). Similar subthermocline oscillations have been described at higher and lower latitudes as potential mechanisms for upward pumping of nitrate

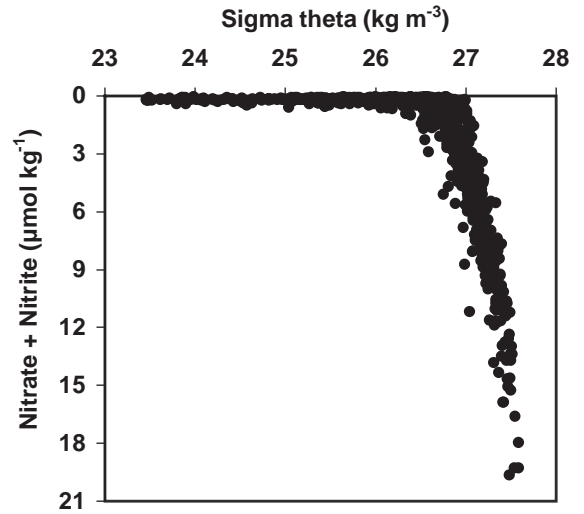


Fig. 9. Nitrate + nitrite ( $\mu\text{mol kg}^{-1}$ ) distribution as a function of  $\sigma_{\theta}$  ( $\text{kg m}^{-3}$ ,  $n = 965$ ). Note the nitrogen trend increasing at densities higher than  $26.0\sigma_{\theta}$ .

(McGillicuddy and Robinson, 1997; Arhan et al., 1998). In the WS, the relatively constant nitracline at depths close to the lower limit of the euphotic zone suggests light limitation of phytoplankton at this level. In the CC, upwelling of deeper waters was found responsible for fertilizing the subsurface (nitrate concentrations  $> 0.5 \mu\text{mol kg}^{-1}$ ), thus increasing the depth-integrated chlorophyll  $a$  (Fig. 6). The CC had a depth-integrated chlorophyll  $a$  ( $31.6 \text{ mg m}^{-2}$ ) significantly higher than the mean of the trade-wind domain ( $23.9 \text{ mg m}^{-2}$ ).

Open oligotrophic oceans often have chlorophyll maxima at depths between 1% and 3% of surface irradiance (Taguchi et al., 1988; Bricaud et al., 1992; Agustí and Duarte, 1999). In the trade-wind domain, the chlorophyll maximum was located at  $\sim 0.8\%$  surface irradiance. Under the assumption of a surface PAR, at noon, of  $410 \text{ W m}^{-2}$ , this percentage corresponds to a value of  $\sim 22 \text{ W m}^{-2}$  over the daylight period which could be small enough to prevent the phytoplankton from reaching deeper nutrient-rich waters. This estimate closely matches observations made at 20°N in the Sargasso Sea of a summer phytoplankton maximum at 120 m depth receiving  $\sim 1\%$  surface irradiance (Bricaud et al., 1992; Jacques and Oriol, 1992; Bahamón, 2002)

representing  $\sim 18 \text{ W m}^{-2}$  over the daylight period. These irradiance values at the chlorophyll maximum are several times higher than the irradiance at higher latitudes, such as in the North Sea, with a summer chlorophyll maximum at 30 m depth receiving 1% surface irradiance ( $\sim 6 \text{ W m}^{-2}$  over the daylight period). In the WS, the DCM is located at a relatively constant distance above the nitracline coinciding with the given estimates of irradiance but independent of isopycnal oscillations. Therefore, the phytoplankton maximum is driven by light limitation rather than by density not only in WS but also in CS and EA. In the CC area, the phytoplankton maximum was found at depths with irradiance around 10% the surface values representing  $\sim 280 \text{ W m}^{-2}$  over the daylight period. This suggests that factors other than light and nutrients control the phytoplankton maximum in this area.

Typical depth-integrated chlorophyll *a* concentrations in the trade-wind domain were around  $24 \text{ mg m}^{-2}$  consistent with estimates given by Goericke and Welschmeyer (1998) for the Sargasso Sea (WS and CS) and Claustre and Marty (1995) for the tropical North Atlantic not only for summer but also for springtime. Relatively, high chlorophyll *a* values were found in CS ( $\sim 32 \text{ mg m}^{-2}$ ) (Fig. 6) indicating the existence, in the open ocean, of chlorophyll *a* rich patches that might not be properly documented from satellite observations because of excessive smoothing. Such patches were not correlated with increasing nitrate fluxes, suggesting that factors other than nitrate are responsible for the chlorophyll increase.

The DCM has been generally linked with diffusive nitrogen fluxes across the thermocline, particularly when the thermocline coincides with the base of the euphotic zone as occurs at high latitudes (Holligan et al., 1984; Sharples et al., 2001). At lower latitudes, a significant correlation between the depths of the thermocline and maximum vertical stability layer (Brunt-Väisälä frequency) and the chlorophyll *a* maximum has been observed in the NW Mediterranean Sea (Velásquez, 1997) and the central Atlantic (Agustí and Duarte, 1999). Other authors attribute the DCM in thermally stratified waters to the diffusive nutrient flux across the nitracline

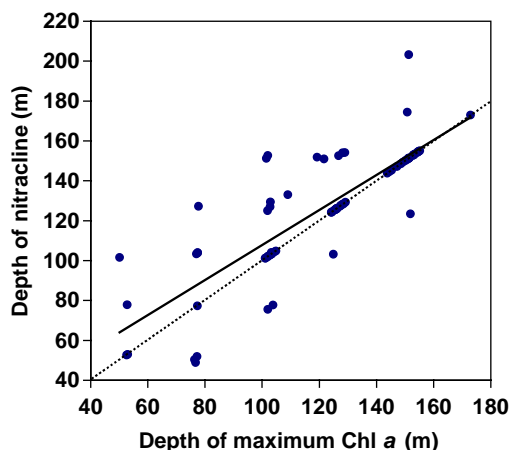


Fig. 10. Relationship between depth of chlorophyll *a* maximum (DCM) and depth of maximum nitrate gradient (DMN) (nitracline) with solid line indicating a linear regression:  $\text{DCM} = 0.8775 (\text{DMN}) + 20.124$  ( $n = 57$ ;  $r^2 = 0.6893$ ;  $p < 0.001$ ). Dashed line represents 1:1 ratio.

(Herbland and Voituriez, 1979; Cullen and Epply, 1981; Longhurst and Harrison, 1989; Varela et al., 1994; Helguen et al., 2002). In the present work, no significant correlations between the depths of the thermocline, the maximum of Brunt-Väisälä frequency, and the chlorophyll *a* maximum were found. Instead, the DCM appears  $\sim 100$  and  $\sim 40$  m below the thermocline in the trade-wind domain and in the CC, respectively, the DCM being closely correlated to the nitracline depth ( $n = 57$ ,  $r^2 = 0.69$ ,  $P < 0.001$ ) (Fig. 10).

In the present work, the density-dependent  $K_z$  together with the nitrate gradients at nitracline were used to compute the upward nitrogen fluxes.  $K_z$  at the nitracline depth was found to increase eastward as the density gradients decrease (except in CC) (Table 1). In the trade-wind domain, the vertical distribution of  $K_z$  was similar to that reported by Lande et al. (1989) for the central North Atlantic. They observed high diffusivity above the pycnocline, lower diffusivity between 50 and 150 m depths, and slightly higher values at 300 m depth. In order to estimate nitrogen fluxes, Planas et al. (1999) gave estimates of turbulent diffusion in the tropical North Atlantic in the range of our estimates in the nitracline ( $\sim 1\text{--}15 \text{ m}^2 \text{ day}^{-1}$ ).

The estimates of nitrate fluxes in the present work were in the range of previous estimates in the tropical North Atlantic. The averages were 0.22, 0.50 and 0.91 mmol N m<sup>-2</sup> day<sup>-1</sup> in the WS, CS, and EA, respectively (Table 1). In the North Atlantic, the upward nitrogen fluxes appear to decrease with latitude. At higher latitudes, in temperate zones of the North Atlantic, Jenkins (1988) estimated 0.6 ± 0.2 mol N m<sup>-2</sup> yr<sup>-1</sup> (1.64 ± 0.55 mmol m<sup>-2</sup> day<sup>-1</sup>) using <sup>3</sup>He. Hurtt and Armstrong (1996) used an ecological model to give estimates of nitrogen flux of ~0.2 mol N m<sup>-2</sup> yr<sup>-1</sup> (0.55 mmol N m<sup>-2</sup> yr<sup>-1</sup>) in the Sargasso Sea, similar to our results. At lower latitudes, in the tropical North Atlantic, estimates of diffusive nitrogen fluxes vary widely. Lewis et al. (1986) estimated an upward nitrogen flux of 0.14 mmol m<sup>-2</sup> day<sup>-1</sup> at 28°N, 23°W, by direct measurements of turbulent diffusion. Planas et al. (1999) gave average estimates of nitrogen flux around 0.74 mmol m<sup>-2</sup> day<sup>-1</sup> along 16–27°N, 28°W, using vertical turbulence parameterization. Gruber and Sarmiento (1997) give nitrate flux estimates of 0.2 mmol m<sup>-2</sup> day<sup>-1</sup> in the tropical and subtropical North Atlantic, based on linear combinations of nitrate and phosphate distribution in the area. This value is similar to our estimates in WS, but lower than the estimates for the whole trade-wind domain (0.53 mmol N m<sup>-2</sup> day<sup>-1</sup>).

The variability of the present estimates of upward nitrogen fluxes in the tropical North Atlantic was explained mainly by the nitrate gradients ( $n = 86$ ,  $r^2 = 0.79$ ,  $P < 0.001$ ), leaving a minor fraction of the variability to the diffusion term ( $n = 86$ ,  $r^2 = 0.12$ ,  $P = 0.001$ ). A similar finding has been reported to take place in the oligotrophic NW Mediterranean Sea (Bahamón and Cruzado, 2003). If it is assumed that new production is in the range of ~1–2 mol C m<sup>2</sup> yr<sup>-1</sup> (Williams and Follows, 1998), our estimates can account for most of it. In the trade-wind domain (WS, CS, EA), the average upward nitrate flux of 0.53 mmol N m<sup>-2</sup> day<sup>-1</sup> (0.19 mol N m<sup>-2</sup> yr<sup>-1</sup>) represents a new production of 1.3 mol C m<sup>2</sup> yr<sup>-1</sup> (assuming a 16:106 N:C Redfield ratio). Planas et al. (1999) found that the nitrate supply in the central Atlantic, similar to our estimates,

is lower than the nitrate uptake by about 0.65 mmol N m<sup>-2</sup> day<sup>-1</sup>, suggesting other sources of nitrate such as the atmosphere.

Assuming total production in the tropical North Atlantic to be ~120 and 180 mg C m<sup>-2</sup> day<sup>-1</sup> in WS + CS and EA, respectively (Sathyendranath et al., 1995; Longhurst et al., 1995), the estimates of net production from this study would imply an  $f$ -ratio (the ratio between nitrate uptake and total nitrogen uptake) of 0.23–0.34. These values are in the high end of the range of 0.1–0.3, typically assumed for the oligotrophic open ocean (Platt and Harrison 1985; McGillicuddy and Robinson, 1997; Planas et al., 1999). In the CC, assuming a total production of 600 mg C m<sup>-2</sup> day<sup>-1</sup> (Longhurst et al., 1995) the estimated new production accounts for only 11% (0.1  $f$ -ratio) of total production well below the estimates of around 64% (0.6  $f$ -ratio) (Minas et al., 1986). This suggests that the upward turbulent diffusion is not responsible for fuelling the new production in this area. In the present work, measured vertical distributions of chlorophyll  $a$  and nitrate (Figs. 3 and 5) suggested that it is mainly horizontal transport that drives new production in the CC.

## 5. Conclusions

The DCM was much deeper than the thermocline. The nitrate concentrations around the thermocline depth were always below the detection limit. Therefore, the diffusive nitrate flux into the euphotic zone was estimated at the nitracline depth. Consequently, the upward nitrate flux appeared to be controlled by diffusion taking place at the top of the nitracline rather than at the thermocline. The top of the nitracline followed the isopycnal distribution in most of the section, except in the WS, where light shortage appears to control the nutrient uptake by phytoplankton at such depths and does not respond to the isopycnal oscillations. Chlorophyll  $a$  patches in WS are linked to fertilization processes related to sub-thermocline instabilities. Other patches located in the center of the open ocean do not respond to isopycnal fronts and fertilization from deeper waters.

The nitrate gradients and the density-dependent turbulent diffusion controlled the spatial variability of the upward nitrate fluxes at the nitracline. The vertical diffusion model reasonably explained the new production in the trade-wind domain (WS, CS, EA) but it could not explain new production in the CC area, where horizontal transport processes driven by the coastal upwelling dynamics supply nutrients.

The division of the tropical North Atlantic into four provinces allowed understanding of some differences in the vertical distribution and concentration of chlorophyll *a*, but did not give support to the expansion of the current division of three to four provinces. Although the concentration at the chlorophyll *a* maximum was statistically similar among the trade-wind provinces, the expected new production from the nitrogen fluxes varied among them. This implies that the relatively homogenous phytoplankton biomass is due to different patterns of *f*-ratio.

### Acknowledgements

WOCE A5 cruise was organized as the Spanish contribution to the global WOCE program. We are grateful to G. Parrilla, cruise leader, and to all members of the scientific team. The support of the *BIO Hespérides* scientific group, officers and crew is also acknowledged. Participation of AC and ZV to the cruise was supported by contract AMB92-1114-E with the Spanish Comisión Interministerial de Ciencia y Tecnología (CICYT). NB was partially assisted with a fellowship from The Spanish Agency for International Co-operation. Improvements suggested by H.E. García, two anonymous referees and the editor are acknowledged.

### References

- Agusti, S., Duarte, C., 1999. Phytoplankton chlorophyll *a* distribution and water column stability in the central Atlantic Ocean. *Oceanologica Acta* 22, 193–203.
- Arhan, M., Mercier, H., Bourlés, B., Gouriou, Y., 1998. Hydrographic sections across the Atlantic at 7°30'N and 4°30'S. *Deep-Sea Research I* 45, 829–872.
- Bahamón, N., 2002. Dynamics of oligotrophic pelagic environments: North Western Mediterranean Sea and subtropical North Atlantic. Ph.D. Thesis, Universitat Politècnica de Catalunya, Barcelona, Spain. 172pp.
- Bahamón, N., Cruzado, A., 2003. Modelling nitrogen fluxes in oligotrophic environments: NW Mediterranean and NE Atlantic. *Ecological Modelling* 163, 223–244.
- Baker, K.S., Frouin, R., 1987. Relation between photosynthetically available radiation and total insolation at the ocean surface under clear skies. *Limnology and Oceanography* 32, 1370–1377.
- Bricaud, A., Morel, A., Tailliez, D., 1992. Mesures optiques. In: Neveux, J. (Ed.), *Les maximums profonds de chl *a* en mer des Sargasses. Données physiques, chimiques et biologiques. Campagne Chlmax. Campagnes Océanographiques Françaises No. 17*, Banyuls-sur-Mer, France, pp. 39–47.
- Claustre, H., Marty, J.-C., 1995. Specific phytoplankton biomasses and their relation to primary production in the tropical North Atlantic. *Deep-Sea Research I* 42, 1475–1493.
- Cullen, J.J., Epply, R.W., 1981. Chlorophyll maximum layers of the southern California Bight and possible mechanisms of their formation and maintenance. *Oceanologica Acta* 4, 23–32.
- Dugdale, R.C., Goering, J.J., 1967. Uptake of new and regenerated forms of nitrogen in primary productivity. *Limnology and Oceanography* 12, 196–206.
- Epply, R.W., Peterson, B.J., 1979. Particulate organic matter flux and planktonic new production in the deep ocean. *Nature* 282, 677–680.
- Furuya, K., 1990. Subsurface chlorophyll maximum in the tropical and subtropical western Pacific Ocean: vertical profiles of phytoplankton biomass and its relationship with chlorophyll *a* and particulate organic carbon. *Marine Biology* 107, 529–539.
- García, H., Cruzado, A., Gordon, L., Escanez, J., 1998. Decadal-scale chemical variability in the subtropical North Atlantic deduced from nutrient and oxygen data. *Journal of Geophysical Research* 103, 2817–2830.
- Gaspar, P., Grégoris, Y., Lefevre, J.-M., 1990. A simple eddy kinetic energy model for simulations of the oceanic vertical mixing: test at station Papa and long-term upper ocean study site. *Journal of Geophysical Research* 95, 16179–16193.
- Goericke, R., Welschmeyer, N.A., 1998. Response of Sargasso Sea phytoplankton, growth rates and primary production to seasonally varying physical forcing. *Journal of Plankton Research* 20, 2223–2249.
- Gruber, N., Sarmiento, J.L., 1997. Global patterns of marine nitrogen fixation and denitrification. *Global Biogeochemical Cycles* 11, 235–266.
- Helguen, S.L., LeCorre, P., Madec, C., Morin, P., 2002. New and regenerated production in the Almeria-Oran front area, eastern Alboran Sea. *Deep-Sea Research I* 49, 83–99.
- Herbland, A., Voituriez, B., 1979. Hydrological structure analysis for estimating the primary production in the

- tropical Atlantic Ocean. *Journal of Marine Research* 37, 87–101.
- Holligan, P.M., Harris, R.P., Newell, R.C., Harbour, D.S., Head, R.N., Linley, E.A.S., Lucas, M.I., Tranter, P.R.G., Weekley, C.M., 1984. Vertical distribution and partitioning of organic carbon in mixed, frontal and stratified waters of the English Channel. *Marine Ecology Progress Series* 14, 111–127.
- Hurtt, G.H., Armstrong, R.A., 1996. A pelagic ecosystem model calibrated with BATS data. *Deep-Sea Research II* 43, 653–683.
- Jacques, N., Oriol, L., 1992. Distribution des chlorophylles et des pheopigments. In: Neveux, J. (Ed.), *Les maximums profonds de Chl a en Mer des Sargasses. Données physiques, chimiques et biologiques. Campagne CHLOMAX. Campagnes Océanographiques Françaises, 17th Edition IFREMER, Banyuls-sur-Mer, France*, pp. 82–98.
- Jeffrey, S.W., Humphrey, G.F., 1975. New spectrophotometric equations for determining chlorophylls *a*, *b*, *c*1 and *c*2 in higher plants, algae and natural phytoplankton. *Biochemisch Physiologie Pflanzen* 167, 191–194.
- Jeffrey, S.W., Welschmeyer, N.A., 1997. Spectrophotometric and fluorometric equations in common use in oceanography. In: Jeffrey, S.W., Mantoura, R.F.C., Wright, S.W. (Eds.), *Phytoplankton Pigments in Oceanography*. UNESCO, France, pp. 597–615.
- Jenkins, W.J., 1988. Nitrate flux into the euphotic zone near Bermuda. *Nature* 331, 521–523.
- Kawase, M., Sarmiento, J.L., 1985. Nutrients in the Atlantic thermocline. *Journal of Geophysical Research* 90, 8961–8979.
- Kiefer, D.A., Kremer, J.N., 1981. Origins of vertical patterns of phytoplankton and nutrients in the temperate open ocean: a stratigraphic hypothesis. *Deep-Sea Research* 28, 1087–1105.
- Lande, R., Li, W.K.W., Horne, E.P.W., Wood, A.M., 1989. Phytoplankton growth rates estimated from depth profiles of cell concentration and turbulent diffusion. *Deep-Sea Research* 36, 1141–1159.
- Lewis, M.R., Harrison, W.G., Oakey, N.S., Hebert, D., Platt, T., 1986. Vertical nitrate fluxes in the oligotrophic ocean. *Science* 234, 870–873.
- Longhurst, R.A., Harrison, G.W., 1989. The biological pump: profiles of plankton production and consumption in the upper ocean. *Progress in Oceanography* 22, 47–123.
- Longhurst, A., Sathyendranath, S., Platt, T., Caverhill, C., 1995. An estimate of global primary production in the ocean from satellite radiometer data. *Journal of Plankton Research* 17, 1245–1271.
- Mayer, D.A., Molinari, R.L., Festa, J.F., 1998. The mean and annual cycle of upper layer temperature fields in relation to Sverdrup dynamics within the gyres of the Atlantic Ocean. *Journal of Geophysical Research* 103, 18545–18566.
- McGillicuddy, D.J., Robinson, A.R., 1997. Eddy-induced nutrient supply and new production in the Sargasso Sea. *Deep-Sea Research I* 8, 1427–1450.
- Menzel, D.W., Ryther, J.H., 1960. The annual cycle of primary production in the Sargasso Sea off Bermuda. *Deep-Sea Research* 6, 351–367.
- Millard, R.C., Owens, W.B., Fofonoff, N.P., 1990. On the calculation of the Brunt–Väisälä frequency. *Deep-Sea Research* 37, 167–181.
- Millero, F.J., Poisson, A., 1981. International one-atmosphere equation of state of seawater. *Deep-Sea Research* 28, 625–629.
- Minas, H.J., Minas, M., Packard, T.T., 1986. Productivity in upwelling areas deduced from hydrographic and chemical fields. *Limnology and Oceanography* 31, 1182–1206.
- Osborn, T.R., 1980. Estimates of the local rate of vertical diffusion from dissipation measurements. *Journal of Physical Oceanography* 10, 83–89.
- Parrilla, G., Lavín, A., Bryden, H., García, M., Millard, R., 1994. Rising temperatures in the subtropical North Atlantic Ocean over the past 35 years. *Nature* 369, 48–51.
- Planas, D., Agusti, S., Duarte, C., Granata, T., 1999. Nitrate uptake and diffusive nitrate supply in the Central Atlantic. *Limnology and Oceanography* 44, 116–126.
- Platt, T., Harrison, W.G., 1985. Biogenic fluxes of carbon and oxygen in the ocean. *Nature* 318, 55–58.
- Sathyendranath, S., Longhurst, A., Caverhill, C.M., Platt, T., 1995. Regionally and seasonally differentiated primary production in the North Atlantic. *Deep-Sea Research I* 42, 1773–1802.
- Schmitz, W.S., McCartney, M.S., 1993. On the North Atlantic Circulation. *Reviews of Geophysics* 31, 29–49.
- Sharples, J., Moore, C.M., Rippeth, T.P., Holligan, P.M., Hydes, D.J., Fisher, N.R., Simpson, J.H., 2001. Phytoplankton distribution and survival in the thermocline. *Limnology and Oceanography* 46, 486–496.
- Taguchi, S., DiTullio, G.R., Laws, E.A., 1988. Physiological characteristics and production of mixed layer and chlorophyll maximum phytoplankton in the Caribbean Sea and Western Atlantic Ocean. *Deep-Sea Research* 35A, 1363–1377.
- Varela, R.A., Cruzado, A., Tintore, J., 1994. A simulation analysis of various biological and physical factors influencing the deep-chlorophyll maximum structure in oligotrophic areas. *Journal of Marine Systems* 5, 1–15.
- Velásquez, Z.R., 1997. *Fitoplancton en el Mediterráneo Noroccidental*. Ph.D. Thesis, Universitat Politècnica de Catalunya, Barcelona, Spain, 271pp.
- Whitledge, T.E., Malloy, S.C., Patton, C.J., Wirick, C.D., 1981. Automated nutrient analyses in seawater. Brookhaven National Laboratory. US Department of Energy and Environment, Upton, NY, 216pp.
- Williams, R.G., Follows, M.J., 1998. The Ekman transfer of nutrients and maintenance of new production over the North Atlantic. *Deep-Sea Research I* 45, 461–489.
- Zakardjian, B., Prieur, L., 1998. Biological and chemical signs of upward motions in permanent geostrophic fronts of the western mediterranean. *Journal of Geophysical Research* 103, 27849–27866.